RSC Advances

ROYAL SOCIETY OF CHEMISTRY

www.rsc.org/advances

Table of Contents

Graphical abstract

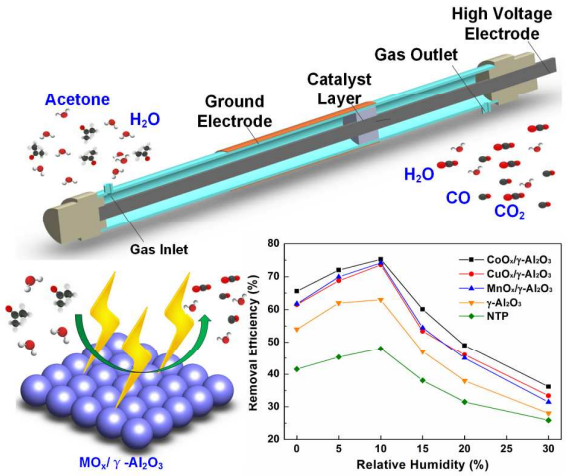

Text:

The gas humidity significantly affects the plasma-catalytic removal of acetone, while the use of catalysts reduces byproducts formation.

Plasma-catalytic removal of low concentration acetone in humid conditions

Xinbo Zhu[1, 2], Xiang Gao[1], Chenghang Zheng[1], Zhihua Wang[1], Mingjiang Ni[1], Xin Tu[2*]*

1 State Key Laboratory of Clean Energy Utilization, Zhejiang University, Hangzhou 310027, China

2 Department of Electrical Engineering and Electronics, University of Liverpool, Liverpool, L69 3GJ, UK

Corresponding Author

Dr. Xin Tu

Department of Electrical Engineering and Electronics

University of Liverpool,

Liverpool L69 3GJ

UK

E-mail: xin.tu@liverpool.ac.uk

Prof. Xiang Gao

State Key Laboratory of Clean Energy Utilization,

Zhejiang University,

Hangzhou 310027,

China

E-mail: xgao1@zju.edu.cn

Graphical abstract

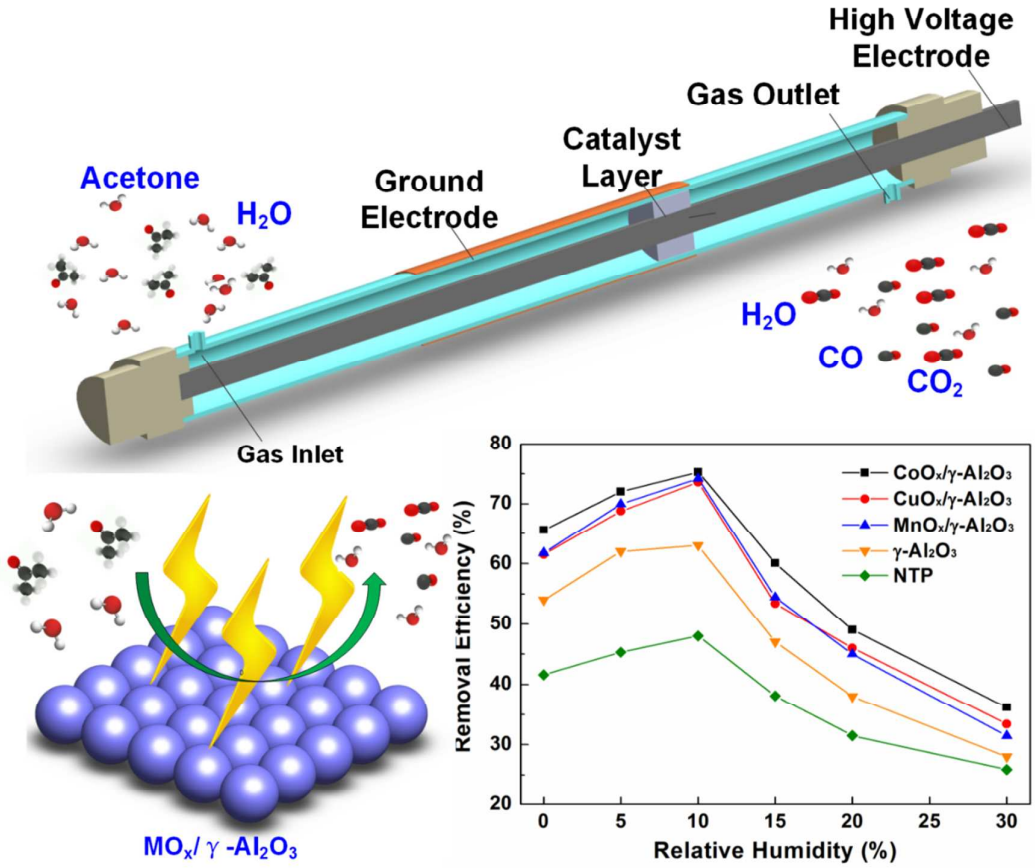

The gas humidity significantly affects the plasma-catalytic removal of acetone, while the use of catalysts reduces byproducts formation.

Abstract

A coaxial dielectric barrier discharge (DBD) plasma reactor has been developed for plasma-catalytic removal of low concentration acetone over MO_x/γ-Al_2O_3 (M = Co, Cu, or Mn) catalysts. The effect of air relative humidity (RH) on the discharge characteristics, acetone removal efficiency, CO_2 selectivity, and byproducts formation with and without catalyst has been investigated. The results show that increasing the RH leads to a decrease of the specific energy density (SED) of the DBD, while packing γ-Al_2O_3 supported metal oxide catalysts into the discharge gap enhances the SED of the discharge. The maximum acetone removal of 75.3% is achieved at an optimum RH of 10% using CoO_x/γ-Al_2O_3 beyond which the removal efficiency of acetone decreases with the increase of the RH. Higher RH inhibits the formation of energetic electrons whistle water can be adsorbed onto the catalyst surface and block active sites on the catalyst surface. It is found that increasing the air humidity enhances both CO_2 selectivity and carbon balance, but decreases the formation of ozone. However, the formation of NO_x slightly increases with increasing the gas humidity. In addition, the presence of these catalysts in the discharge significantly decreases the formation of unwanted byproducts (O_3 and NO_x) and promotes the deep oxidation of acetone towards CO_2 with an increased carbon balance.

Keywords: Dielectric barrier discharge, Non-thermal plasma, Plasma-catalysis, Acetone removal; Humidity

1. Introduction

With the rapid development of industry and economy, volatile organic compounds (VOCs) pollution has become the focus of global attention because of the position of VOCs as the main pollution source and their negative impact on both environment and public health.[1, 2] VOCs have also been identified as the major precursors for the formation of $PM_{2.5}$ and photochemical smog. Exposure to VOCs may cause irritation, headache, dizziness and even cancer. Conventional VOC abatement technologies, such as adsorption, absorption, catalytic oxidation/combustion, are not cost-effective when dealing with the degradation of low concentration VOCs in high volume waste gas streams.[3] In the past two decades, non-thermal plasma technology has been identified as a promising and alternative route for gas cleaning and purification with unique advantages of low energy cost, mild working conditions, system compactness, high reaction rate and fast response, and easy operation.[4-6] Non-thermal plasmas can generate various kinds of species including highly energetic electrons and chemically active species (e.g. radicals, excited atoms, molecules and ions) for the initiation and propagation of physical and chemical reactions. Non-thermal plasma has a distinct non-equilibrium character, which means that the overall plasma gas temperature can be as low as room temperature, while the electrons are highly energetic with a typical average electron temperature of 1-10 eV. As a result, non-thermal plasma can easily break most chemical bonds of molecular pollutants at low temperatures and convert gas pollutants into end-products including CO, CO_2, H_2O and some unwanted byproducts (e.g. NO_x).[7, 8]

However, the use of a plasma discharge alone leads to the formation of high concentration unwanted byproducts and low selectivity of desirable final products. The combination of non-thermal plasma with catalysis has been demonstrated to be very effective for the removal of low concentration gas pollutants in high volume waste gas streams. Our previous work has shown that the presence of solid catalysts (e.g. TiO_2) in the plasma significantly changes the electron energy distribution with an increase in electron density in the high energy tail of the distribution function, which in turn affects plasma chemical reactions.[9] It is well recognised that the synergistic effect of

plasma-catalysis could be generated through the effective interactions between the plasma and catalyst, which can activate catalysts at low temperatures and significantly improve the reaction performance in terms of the removal efficiency and energy efficiency, whilst inhibit or reduce the formation of unwanted byproducts.[10-13] Up until now, various kinds of precious and transition metals have been tested as the active metal phase for the removal of VOCs in plasma-catalytic reactions. Kim et al.[14] investigated the effect of supported metal (Ag, Ni, Pt, and Pd) catalysts with different metal loadings on the decomposition of benzene in a flow-type dielectric barrier discharge (DBD) reactor. They found that the supported Ag catalysts showed the best performance for the removal of benzene, and the type of catalyst significantly affects the carbon balance, CO_2 selectivity and the formation of ozone and NO_x. Hakoda et al.[15] reported that Ag/TiO_2 exhibited the highest removal efficiency in xylene decomposition among TiO_2 supported Mn, Ag, Au and Pt catalysts. Raju et al.[16] developed metal modified sintered metal fiber (SMF) electrodes for the oxidation of mixture VOCs (xylene, cyclo-hexane and n-hexane) in a DBD reactor. Both Co and Mn modified SMF inner electrodes exhibited a remarkable enhancement in removal efficiency. Compared to noble metal catalysts, supported transition metal catalysts have gained increasing interest due to their low cost and comparable efficiency for the destruction of VOCs in waste gas streams.

Previous works reported that the generation of synergistic effect in plasma-catalytic removal of VOCs depends on a wide range of plasma processing parameters, such as initial concentration of pollutants[17], carrier gas composition[18], gas flow rate[19] and plasma power supply.[20, 21] However, most of these reactions were carried out in ideal processing conditions (e.g. simulated dry air or pure N_2) without taking into account the relative humidity of carrier gas. From an industrial application point of view, gas humidity is one of the most important factors affecting the synergy of plasma-catalysis and the energy efficiency of plasma processing since waste gases from industrial VOC emission sources generally contain water. The effect of gas humidity on the removal of VOCs in a plasma-catalysis system is even more complex. Recent review paper has pointed out that the influence of gas humidity on the plasma-catalytic removal of VOCs is poorly investigated in the literature.[22] The

presence of high concentration water vapor in a plasma-catalysis system may cover the active sites on the catalyst surface and reduce the formation of ozone and O atoms, both of which play an important role in the plasma-catalytic oxidation of VOCs.[23] Huang et al. found the use of water vapor could inhibit the removal of toluene in the plasma process combined with TiO_2 or MnO_x. They reported an optimum water vapor content for achieving the highest CO_2 selectivity and carbon balance.[24] Fan et al.[25] evaluated the effect of different humidity levels on the destruction of benzene, toluene and xylene (BTX) using plasma-MnO_x/Al_2O_3. The decomposition of BTX was inhibited by the presence of both water vapor and ozone. Wu et al.[26] found the presence of water vapor in a combined plasma-catalysis system could significantly reduce the efficiency for toluene removal over Ni-based catalysts. Sugasawa et al. showed that no-rate promoting effect of water was observed in the decomposition of $PhCH_3$, CH_2Cl_2 and CH_3OH in a packed bed DBD reactor and the presence of water (0.5% - 2%) increased CO_2 selectivity and carbon balance to different degrees, depending on the type of gas pollutants. However, they found that high humidity level can have both positive and negative effects on the removal of $PhCH_3$.[27] These findings suggest that the effect of gas humidity on the removal of VOCs may also depend on the chemical structure of VOC molecules. Currently, there is very limited work focused on the destruction of acetone using non-thermal plasmas due to its relative stable chemical structure,[28-31] while the use of transition metal supported catalysts for plasma-induced removal of acetone has not been studied before. In addition, the investigation of the effect of gas humidity on the plasma-catalytic removal of acetone is totally missing.

From our perspective, a better understanding of acetone decomposition process especially in the presence of water vapor is essential for optimising the plasma-catalytic process. A typical coaxial DBD reactor has been developed for the plasma-catalytic removal of acetone over MO_x/γ-Al_2O_3 (M = Cu, Co, or Mn) at atmospheric pressure and low temperatures. The effect of the RH on the discharge characteristics, acetone removal efficiency, CO_2 selectivity, carbon balance, and the formation of O_3 and NO_x (NO_2 and N_2O) has been investigated in the absence and presence of the

catalysts.

2. Description of the experiments and the model

2.1 Experimental setup

Fig. 1 shows the schematic diagram of the experimental setup. A 100 mm-long copper foil (ground electrode) was wrapped over a quartz tube with an inner diameter of 20 mm and wall thickness of 2.5 mm. A stainless steel rod with an outer diameter of 16 mm was placed in the axial centre of the quartz tube and acted as a high voltage electrode. As a result, the length of the discharge zone is 100 mm with a discharge gap of 2 mm. The DBD reactor was supplied by an AC high voltage power supply with a maximum peak voltage of 30 kV and a frequency of 50 Hz. In this study, simulated dry air was used as carrier gas. Water vapor with a relative humidity between 0 and 30 % was introduced into the plasma reactor by passing a dry nitrogen flow through a water bubbler kept in an ice-water bath (0 °C). A standard gas cylinder containing 2000 ppm acetone (N_2 balanced) was used to introduce acetone into the plasma reactor with a constant initial acetone concentration of 200 ppm. The total flow rate for all the experiments was kept at 200 mL/min, corresponding to a gas residence time of 1.13 s. A fibre optical thermometer (Omega, FOB102) was used to measure the plasma temperature (25-35 °C) in the discharge area.

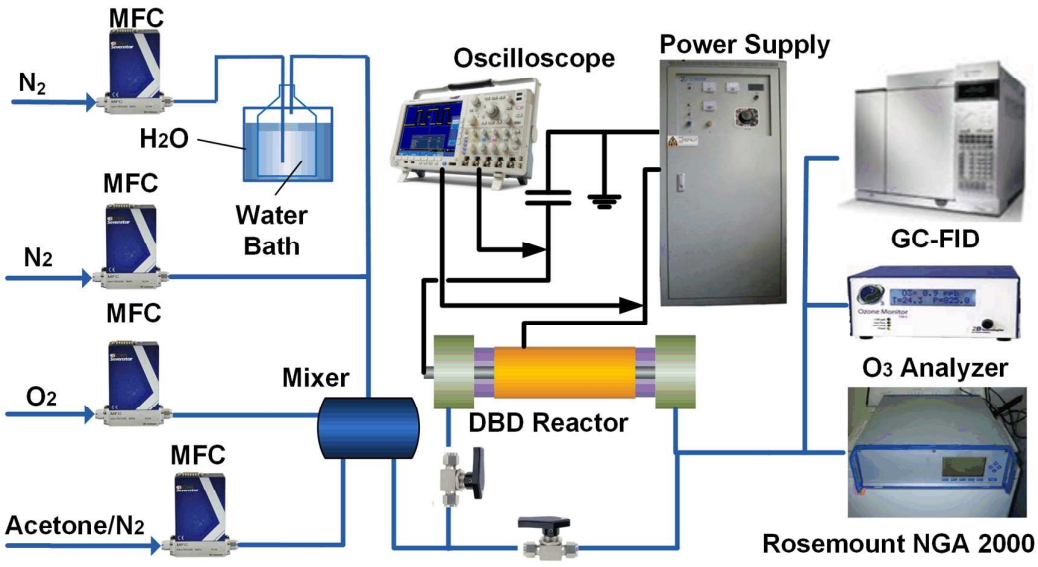

Fig. 1. Schematic diagram of the experimental setup.

The $MO_x/\gamma\text{-}Al_2O_3$ (M = Mn, Cu, or Co) catalysts with a metal loading of 10 wt % were prepared by impregnation of aqueous solution of nitrate salts $Mn(NO_3)_2$, $Co(NO_3)_2$, and $Cu(NO_3)_2$ (AR, 99.5%, Aladdin Reagents Ltd). The $\gamma\text{-}Al_2O_3$ support was calcined at 500 °C for 2h prior to use. The aqueous precursor salt solutions were prepared and stirred steadily for 2h at room temperature, and then the support ($\gamma\text{-}Al_2O_3$) was added to the solutions and dried in a water bath at 80 °C for 6h. All samples were calcined at 500 °C for 5h and sieved to 20-40 mesh. The obtained samples were denoted as $MnO_x/\gamma\text{-}Al_2O_3$, $CoO_x/\gamma\text{-}Al_2O_3$ and $CuO_x/\gamma\text{-}Al_2O_3$, respectively. For the plasma-catalytic chemical reactions, the catalysts were packed into the discharge gap and held by glass wool.

A high voltage probe (Tektronix, P6015A, 1000:1) was used to measure the applied voltage of the discharge, while a Tektronix P5100 probe was used to measure the voltage across the external capacitor C_{ext} (1μF), which was connected between the reactor and the ground. All the electrical signals were monitored by a digital oscilloscope (Tektronix 3034B). The Q-U Lissajous method was used to calculate the discharge power (P) of the DBD reactor, which is proportional to the area of the Lissajous diagram:

$$P = f \cdot C_{ext} \cdot A$$

where C_{ext} is the capacitance of the external capacitor, f is the frequency and A is the area of the Lissajous diagram. The discharge power of the plasma reactor can be controlled in real time by a customised software.

The specific energy density (SED) is defined as the energy deposited per unit volume of the gas flow:

$$SED\ (J/L) = \frac{P(W)}{Q(L/min)} \times 60$$

where Q denotes the total gas flow rate (in *L/min)*.

The concentration of acetone before and after the plasma reaction was measured by a gas chromatograph (Agilent 7890A) with a flame ionisation detector (FID) and a 30 m × 0.25 mm HP - INNOWAX capillary column. The oven temperature was kept at constant (60 °C). The concentration of CO_x and NO_x were monitored by a Rosemount NGA2000 FTIR gas analyzer, while ozone was measured by an UV ozone monitor (2B Technology).

In this study, the removal efficiency of acetone ($\eta_{acetone}$), carbon balance and CO_2 selectivity are defined as follows:

$$\eta_{acetone}(\%) = \frac{c_{in}-c_{out}}{c_{in}} \times 100\%$$

$$\text{carbon balance } (\%) = \frac{c_{co}+c_{co_2}}{3(c_{in}-c_{out})} \times 100\%$$

$$\text{CO}_2 \text{ selectivity } (\%) = \frac{c_{co_2}}{3(c_{in}-c_{out})} \times 100\%$$

where c_{in} and c_{out} are the concentration (in ppm) of acetone before and after the plasma reaction, respectively; c_{co} and c_{co_2} denote the concentration of produced CO and CO_2.

2.2 Description of the model

In this model, a Boltzmann equation solver (BOLSIG+) based on the classical two-term approximation was used to calculate the electron energy, rate coefficients and energy fraction of electron impact reactions.[32, 33] The chemistry set (see Table S1 in Electronic Supplementary Information) used in this model consisted of 51 electron impact reactions involving the carrier gas (N_2, O_2 and H_2O), while acetone was excluded in the model due to its low concentration. The cross sections of N_2, O_2 and H_2O were obtained from the references.[34-36] In a typical air DBD, the electron density of the discharge is in the range of 10^{18}-10^{21} m^{-3}.[37, 38] An electron density of 10^{19} m^{-3} and reduced electric field (150 Td) were used for the calculation,[39, 40] while the temperature was set as 300 K in this model. An estimated uncertainty of the calculation is around 5%.

The formulas used to calculate the rate coefficient and energy fraction (EF) are listed as follows:

$$k_i = \gamma \int_0^\infty \varepsilon \sigma_i F_0 d\varepsilon$$

For elastic reactions,

$$k_{EF,i}\ (\%) = \frac{2m}{M_i} \gamma \int_0^\infty \varepsilon^2 \sigma_i F_0 d\varepsilon$$

For inelastic reactions,

$$k_{EF,i}\ (\%) = u_i k_i$$

$$EF_i = \frac{x_i k_{EF,i}}{\sum_{i=1}^{N} x_i k_{EF,i}} \times 100\ \%$$

where k_i is the rate coefficient of the i[th] reaction, $\gamma = (2e/m)^{1/2}$ is a constant, ε is the electron energy in eV, σ_i is the total cross section of the i[th] reaction, F_0 is the energy distribution, $k_{EF,i}$ is the energy fraction coefficient for the i[th] reaction, u_i is the threshold of i[th] collision reaction and x_i is the mole fraction of the i[th] species, EF_i is the energy fraction of the i[th] reaction. It is worth noting that the energy fraction of the reactions depends on the gas composition.

3. Results and Discussion

3.1 Discharge Characteristics

Fig. 2 shows the effect of RH and γ-Al_2O_3 pellets on the specific energy density of the air discharge at a constant applied voltage of 13 kV. Clearly, increasing the gas humidity significantly decreases the SED of the air discharge regardless the presence of γ-Al_2O_3 pellets. At a fixed applied voltage of 13 kV, with the increase of the RH from 0 (dry air) to 30%, the SED of the air discharge without packing decreases from 441.2 J/L to 405.8 J/L, while this value drops from 499.3 J/L to 448.4 J/L when γ-Al_2O_3 pellets are packed into the discharge gap. In addition, the SED of the air discharge packed with MO_x/γ-Al_2O_3 catalysts (M = Cu, Co or Mn,) is almost same as that of the discharge combined with γ-Al_2O_3 pellets due to a low metal oxide loading (10 %). Packing these catalysts into the discharge gap is found to enhance the SED of the air discharge by 10.4-13.6% at the same applied voltage. Similar behaviour was reported in previous literatures.[41, 42]

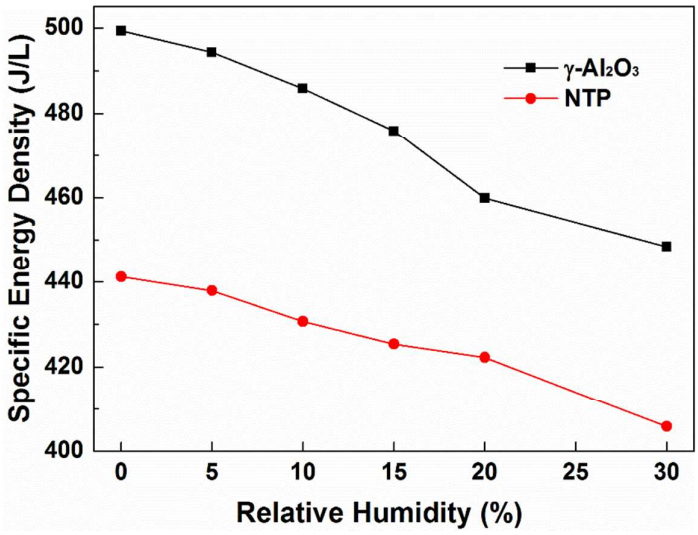

Fig. 2. Effect of RH on the specific energy density of the air discharge a constant applied voltage of 13 kV.

It is well recognised that introducing water vapor into the plasma could change the discharge

characteristics since water can trap energetic electrons via electron impact dissociative attachment due to its electronegativity property [43]:

$$e + H_2O \rightarrow OH + H^- \qquad R1$$

The attachment coefficient of this reaction (R1) in plasmas depends on both electric field strength and water content.[44, 45] Water has a higher attachment coefficient compared to N_2 and O_2, which suggests that increasing gas humidity could increase the probability of electron attachment reaction at a constant applied voltage. Meanwhile, the discharge volume and the number of micro-discharge in the air discharge are reduced.[46]

Previous works have demonstrated that packing catalyst pellets into the discharge gap generates a non-uniform electric field with enhanced local electric field strength near the contact points between the pellets and pellet-wall.[9] Compared to the plasma without catalyst, the integration of plasma and solid catalysts shifts the discharge behaviour from dominant filamentary discharges to a combination of surface discharges on the catalyst surface and filamentary discharges in the void space between the pellets and pellet-wall.[47] In the humid air plasma-catalysis system, both filamentary discharges and surface discharges could be inhibited due to higher electron attachment probability and lower ion mobility caused by the adsorption of water onto the catalyst surface.[48]

3.2 Acetone Oxidation

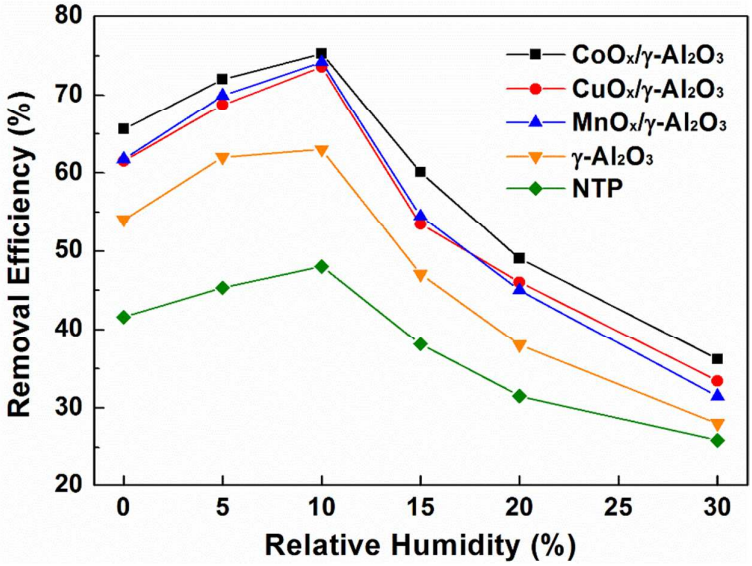

Fig. 3. Effect of RH on the removal efficiency of acetone in the air discharge with and without catalyst at a SED of 500 J/L.

Fig. 3 shows the influence of water vapor on the removal of acetone using plasma with and without catalyst at a constant SED of 500 J/L. Clearly, acetone removal efficiency is significantly affected by the gas humidity. In the plasma process without catalyst, acetone removal efficiency increases from 41.6% in dry air to 48.2% at 10% RH, then it falls to 25.9% at a RH of 30%. For the plasma reactions combined with these catalysts, the removal efficiency of acetone follows the same trend, peaked at a RH of 10% before decreasing with the increase of the humidity, which suggests the decrease of the acetone decomposition with the increase of the RH (> 10%) might only be attributed to the air humidity. The results also show that an optimum water vapor concentration exists for obtaining a maximum removal efficiency of acetone in the plasma process irrespective of the presence of catalyst. Similar phenomenon was observed in previous studies where an optimum water contend of around 20% was found for the removal of both TCE and toluene.[6]

Packing the $MO_x/\gamma\text{-}Al_2O_3$ catalysts into the discharge gap significantly enhances the removal efficiency of acetone by 48% - 56%. The synergistic effect of plasma-catalysis for acetone removal is found to be prominent at a low gas humidity (< 10%). The removal efficiency of the plasma

process in the tested RH range follows the order $CoO_x/\gamma\text{-}Al_2O_3 > CuO_x/\gamma\text{-}Al_2O_3 \approx MnO_x/\gamma\text{-}Al_2O_3 > \gamma\text{-}Al_2O_3 >$ plasma only. Compared to the plasma destruction of acetone, the presence of $\gamma\text{-}Al_2O_3$ in the discharge enhances the removal efficiency of acetone. It is believed that $\gamma\text{-}Al_2O_3$ provides an oxidative environment for surface chemical reactions to take place upon, as well as having a large surface area and Lewis acid sites. The catalytic performance of $\gamma\text{-}Al_2O_3$ for acetone destruction can be further improved by the addition of a small amount of metal oxides since the loading of metal oxides on $\gamma\text{-}Al_2O_3$ enhances the redox properties of the catalysts, which are favourable for the oxidation of VOCs on the catalyst surface.[49] Similar phenomenon was reported in the plasma-catalytic oxidation of CH_2Cl_2 and benzene.[50, 51] Subrahmanyam et al. reported the CoO_x based catalysts exhibited the better performance than MnO_x for the oxidation of toluene in a DBD reactor,[52] while Wu et al. found that $CuO/\gamma\text{-}Al_2O_3$ and $MnO_x/\gamma\text{-}Al_2O_3$ showed the similar catalytic activity for the removal of toluene in a DBD reactor.[53] These findings are in a fairly good agreement with our experiment results.

It is believed that VOC molecules can be decomposed by non-thermal plasmas via two main pathways: (a) electron impact reactions; (b) reactions induced by heavy species (e.g., radicals and excited species).[42] To get new insight into the effect of the gas humidity on the potential reaction mechanisms for the removal of acetone, mean electron energy and energy fraction for the main electron impact reactions in a single micro-discharge was calculated using BOLSIG+. Fig. 4a shows the calculated mean and maximum electron energy as a function of the relative humidity. The mean electron energy (from 4.126 eV in dry air to 4.088 eV in humid air with a RH of 30%) is almost independent on the humidity level between 0 and 30%, while the maximum electron energy of the discharge decreases from 44.60 to 39.29 eV with the increase of the humidity from 0 to 30%. The electrons have sufficient energy to generate chemically reactive species in the humid air plasma through electron impact reactions such as excitation, dissociation and ionisation. OH is one of the most important radicals for the oxidation of gas pollutants in humid air plasmas, which can be generated by electron impact dissociation of water R2 or by R5 and R6. The main reaction

pathways for OH generation in the humid air plasma are listed as follows:[6]

$e + H_2O \rightarrow OH + H + e$ R2

$e + N_2 \rightarrow N_2(A) + e$ R3

$e + O_2 \rightarrow e + O + O(1D)$ R4

$N_2(A) + H_2O \rightarrow N_2 + OH + H$ R5

$O(1D) + H_2O \rightarrow 2OH$ R6

Fig. 4b shows the reaction rate coefficient of three reactions (R2-R4) is slightly decreased as the RH increases from 0 to 30%. For instance, the rate coefficient of R2 decreases from 3.894×10^{-16} m^3s^{-1} in the dry air plasma to 3.791×10^{-16} m^3s^{-1} in the DBD with a RH of 30%. Previous work also showed that no-rate promoting effect of water was observed in the decomposition of $PhCH_3$, CH_2Cl_2 and CH_3OH in a packed bed DBD reactor.[27] At higher RH, the rotational and vibrational excitation of H_2O plays a more important role in electron impact reactions due to their large cross sections and low threshold energy, which consumed energetic electrons.[36] However, regarding the carrier gas concentrations and the reaction coefficient of R2-R4, more OH radicals could be produced in a single micro-discharge at higher RH while the populations of N_2 (A) and O (1D) remain almost constant.

Fig. 4c shows the energy fraction of R2-R4 in the plasma processing of acetone. The energy fraction of R2 slightly increases from 0 to 0.11% when the RH changes from 0 to 30%. Thus more energy can be used to generate OH radicals in a single micro-discharge for the oxidation of gas pollutants at higher gas humidity. It is worth noting that the products of R3 and R4, namely N_2 (A) and O (1D), can be used to generate OH radicals via R5 and R6. The energy fractions of R3 and R4 are kept almost constant with the change of the RH. In addition, N_2 (A) and O (1D) can react with acetone molecules directly.

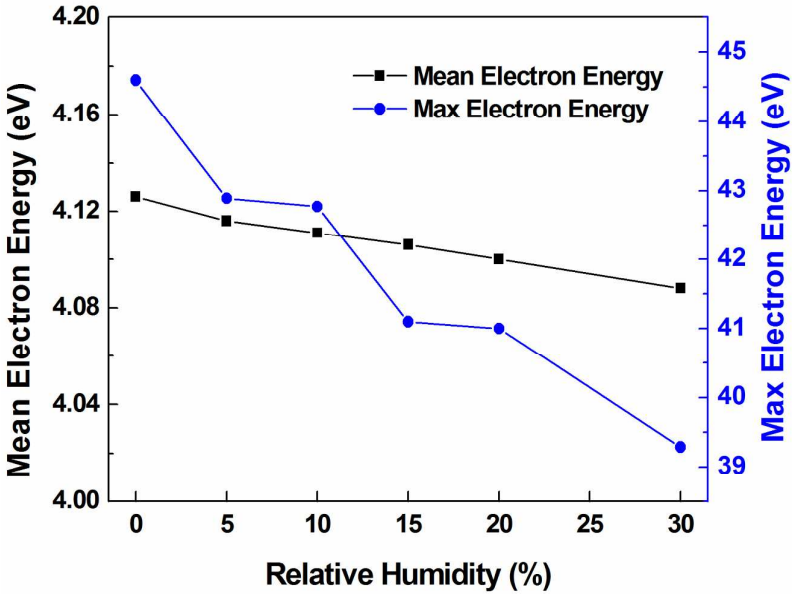

(a)

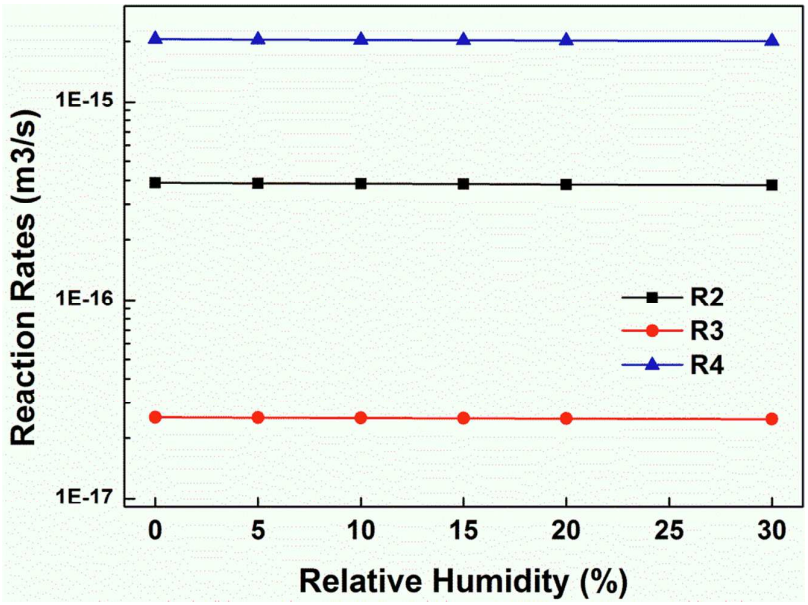

(b)

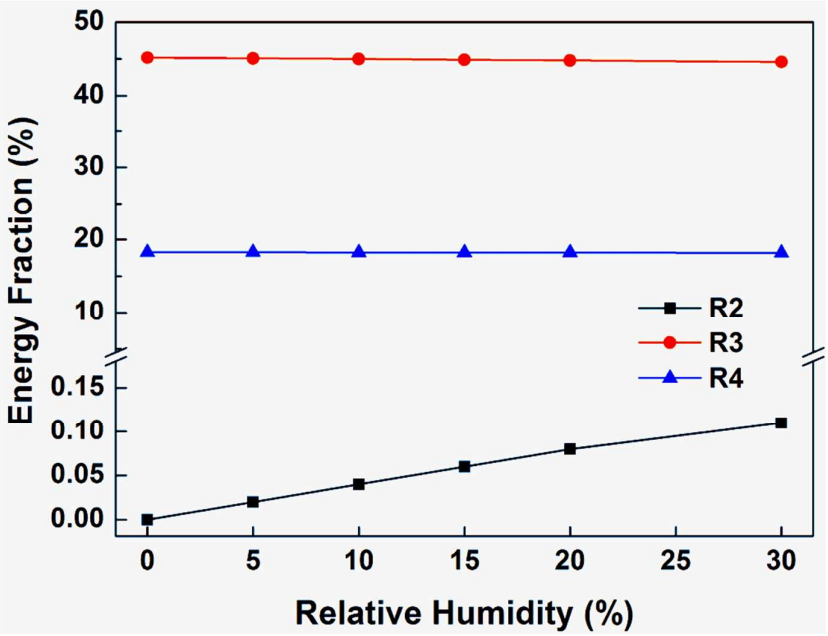

(c)

Fig. 4. (a) Calculated mean and maximum electron energy in the humid air discharge as a function of the RH under 150 Td; (b) reaction rate of R2-R4 vs. relative humidity; (c) energy fraction of R2-R4 vs. relative humidity.

OH plays a more important role than O radicals in the oxidation of acetone since the reaction rate of acetone oxidation with OH (2.22×10^{-13} $cm^3mol^{-1}s^{-1}$) is three orders of magnitude higher than that of the reaction with O (7.54×10^{-16} $cm^3mol^{-1}s^{-1}$).[54, 55] In the humid air discharge, the generated OH radicals could accelerate the reaction for the oxidation of acetone, resulted in a higher removal efficiency. On the other hand, the presence of water vapor in the plasma has a negative effect on the plasma-catalytic acetone oxidation due to the electronegativity of water. Increasing the air humidity reduces the number of micro-discharges in the DBD and quenches energetic electrons and metastable species for acetone decomposition. In this work, the negative effect becomes more significant at a relative humidity of >10%, which leads to the decrease in removal efficiency. There is an optimum humidity (10% in this work) to balance these two inverse effects in the plasma destruction of acetone.

In the DBD reactor packed with catalysts, the acetone removal process is also sensitive to the RH since both plasma physical process and plasma–assisted catalytic surface reactions are affected by the gas humidity. Adsorption of VOC molecules onto catalyst surface has been considered as a key and essential step in plasma-assisted catalytic reaction. Water molecules can also be adsorbed on catalyst surface by van der Waals force.[56] The competitive adsorption on catalyst active sites between gas pollutants and water molecules could negatively affect the interaction between the VOC and catalysts. At a low RH (< 10%), only limited active sites on the catalyst surface are covered by water and H_2O molecule monolayer is not formed. As the bond energy of H_2O decreases,[57] the adsorbed water molecules may be used to form OH and HO_2 radicals, both of which contribute to the improvement of acetone removal efficiency. With increasing the RH (>10%), the presence of H_2O would cover or block more active sites on the catalyst surface,[23] which reduces the catalyst activity and inhibits the adsorption of acetone on the catalyst surface. Deng et al. reported the presence of water on the catalyst surface could form one or more H_2O molecule monolayer, depending on the relative humidity. They found that the first H_2O molecule monolayer with a thickness of 0.3 nm was formed at a RH of ~15%, while the second water layer was generated at a RH of 35-40%.[58] In this study, the adsorption of acetone molecules onto the catalyst surface are significantly inhibited when the air humidity is higher than 10%, leading to a dramatically decrease in the removal efficiency of 39.1%, 40.2%, 42.7% and 35% for CoO_x/γ-Al_2O_3, CuO/γ-Al_2O_3, MnO_x/γ-Al_2O_3 and γ-Al_2O_3, respectively as the RH increases from 10% to 30%. However, in the absence of a catalyst, the removal efficiency of acetone is only decreased of 25.9% when the RH changes from 10% to 30%.

3.3 CO_2 Selectivity and Carbon Balance

CO and CO_2 are found to be the main gas products of acetone removal in the DBD with and without catalyst. The influence of the humidity and catalysts on the selectivity of CO_2 is plotted in Fig. 5. Clearly, water vapor has a significant effect on CO_2 selectivity at a low RH (<15%). In the

absence of a catalyst, CO_2 selectivity is increased by 43.9% from 41.9% to 60.3% from dry air to humid air with 15% RH, followed by the saturation between 15% and 30%. Similar observations were reported in previous studies.[24] Our recent work has demonstrated that electrons and $N_2(A)$ play a dominant role in the decomposition of acetone in a DBD reactor, while the oxidative radicals make a significant contribution to the deep oxidation of byproducts into CO and CO_2.[59] The presence of OH radicals could react with acetone (R7) and promote CO oxidation via the exit (R8).

$$OH + CH_3COCH_3 \rightarrow H_2O+CH_3COCH_2 \qquad R7$$

$$CO + OH \rightarrow CO_2 + H \qquad R8$$

As mentioned in section 3.2, more OH radicals can be formed in a single micro-discharge with increasing the RH, whereas the number density of electrons and micro-discharges could be limited by the attachment of water molecules with increasing RH. These two effects might lead to the saturation of OH radicals at higher RH.

The effect of catalysts on CO_2 selectivity has also been investigated. In the presence of a catalyst inside the plasma, similar evolution of CO_2 selectivity as a function of the RH can be observed. Packing MO_x/γ-Al_2O_3 catalysts into the discharge gap is found to significantly enhance the selectivity of CO_2, which can be attributed to the oxidation of acetone on the catalyst surface by oxidative radicals. In the humid air plasma, due to the van der Waals interactions, water can be adsorbed onto catalyst surfaces and blocks catalytic active sites, especially at a high humidity (> 15%), which leads to the saturation of CO_2 selectivity. The enhancement of CO_2 selectivity can be attributed to the formation of OH radicals on/near the catalyst surface However, CO_2 selectivity is weakly dependent on the composition of the catalysts. Note that the selectivity of CO_2 in the DBD combined with these catalysts is much higher than that in the case of packing catalyst support (γ-Al_2O_3).

The influence of the gas humidity on the carbon balance is plotted in Fig. 5b. Similarly, the presence of water vapor improves the carbon balance for all the tested operating conditions. The carbon balance increases with the increase of the RH from 0 to 30%. In the plasma process with a

low RH, organic byproducts including CH_4, HCHO, HCOOH, HCN and some N-containing organics were detected, which suggests a poor mineralisation of acetone with a low carbon balance. The formation of organic byproducts was significantly reduced when MO_x/γ-Al_2O_3 catalysts or γ-Al_2O_3 support were placed in the discharge area. The presence of the catalysts in the plasma leads to the generation of more chemically active species such as O atoms and promotes the oxidation of byproducts on the catalyst surface. Interestingly, no nitrogen-containing byproducts were detected in the plasma-catalytic destruction of acetone.

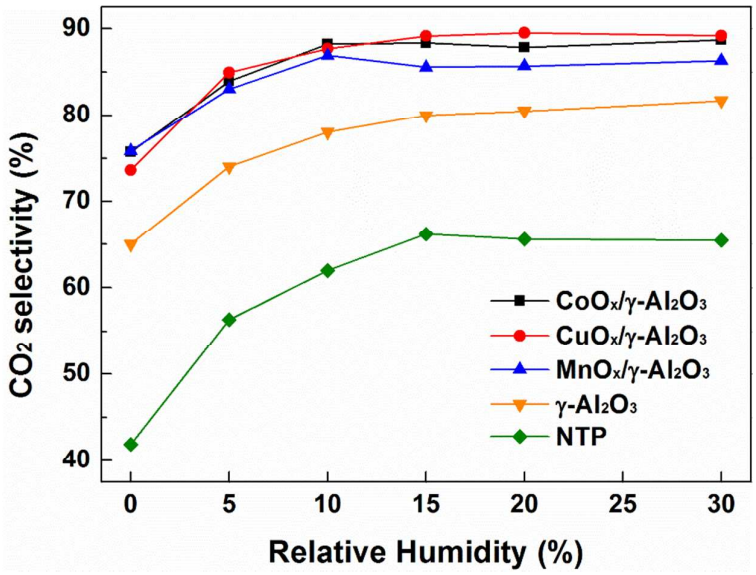

(a)

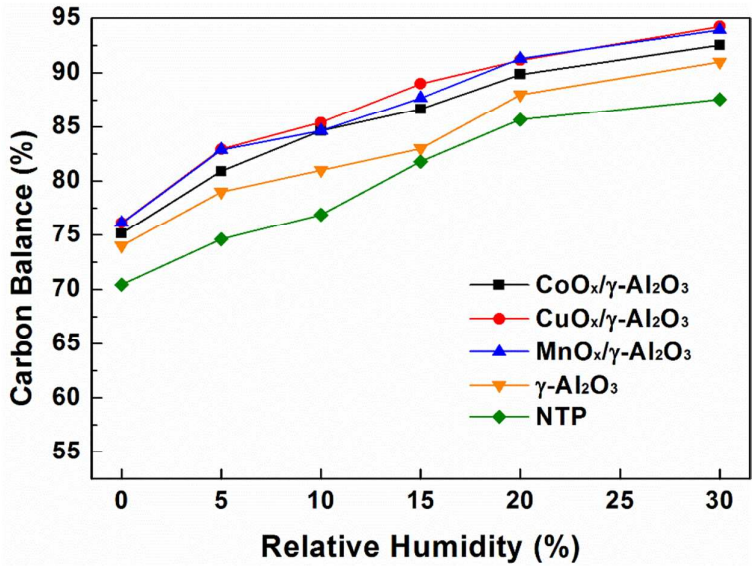

(b)

Fig. 5. Effect of RH on (a) CO_2 selectivity and (b) carbon balance.

3.4 Byproducts Formation

3.4.1 Ozone formation

Ozone, as one of the most important inorganic byproducts in plasma process, is mainly formed by three-body recombination of atomic oxygen and molecular oxygen via

$$O + O_2 + M \rightarrow O_3 + M \qquad R9$$

In the air plasma, the third body M can be nitrogen or oxygen molecules. Here atomic oxygen is generated via electron impact dissociation of oxygen:

$$e + O_2 \rightarrow e + O + O \qquad R10$$

The effect of the RH on ozone formation in the effluent is presented in Fig. 6. In the absence of a catalyst, the ozone concentration decreases from 693 to 460 ppm with the increase of the RH from 0 to 30%. Packing the catalysts into the discharge gap shows the same trends, but significantly reduces the ozone concentration. The ozone concentration follows the order: plasma alone > γ-Al_2O_3 > CoO_x/γ-Al_2O_3 > CuO/γ-Al_2O_3 > MnO_x/γ-Al_2O_3. Similar observations were reported in previous works.[60] The presence of MnO_x catalyst pellets in the plasma leads to a lowest ozone concentration in the plasma-catalytic decomposition of acetone. As reported by Dhandapani et al.[61], MnO_2 is more effective to decompose ozone compared to other metal oxide catalysts, which can explain why the ozone content in the plasma-MnO_x/γ-Al_2O_3 system is the lowest under the same operating conditions. In the humid air plasma, highly energetic electrons can be trapped by water due to the electronegativity of water. Both OH radicals and H_2O will react with atomic oxygen via R11 and R12. Both energetic electrons and atomic oxygen are the precursor for ozone formation. Chen et al.[62] examined the effect of water on the ozone generation and found OH radicals can directly react with ozone via R13. These confirm that the gas humidity could inhibit the formation of ozone.

$H_2O + O \rightarrow OH + OH$ R11

$O + OH \rightarrow O_2 + H$ R12

$OH + O_3 \rightarrow O_2 + HO_2$ R13

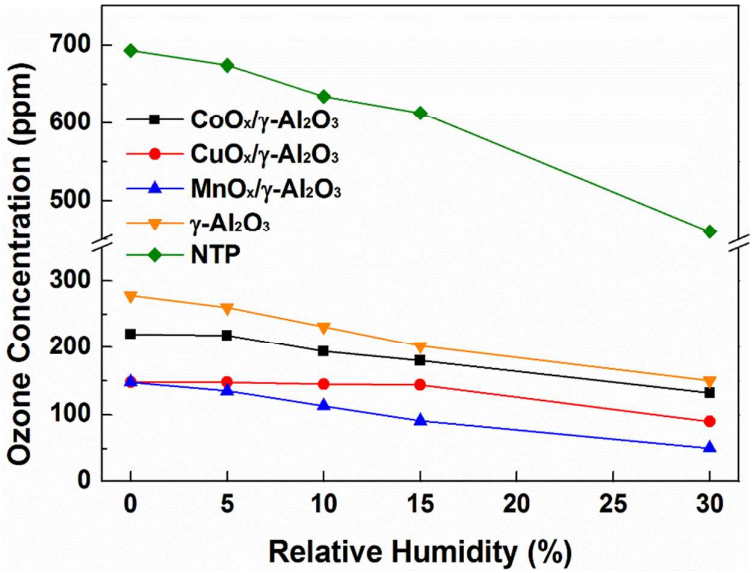

Fig. 6. Effect of RH on ozone formation.

3.4.2 NO_x formation

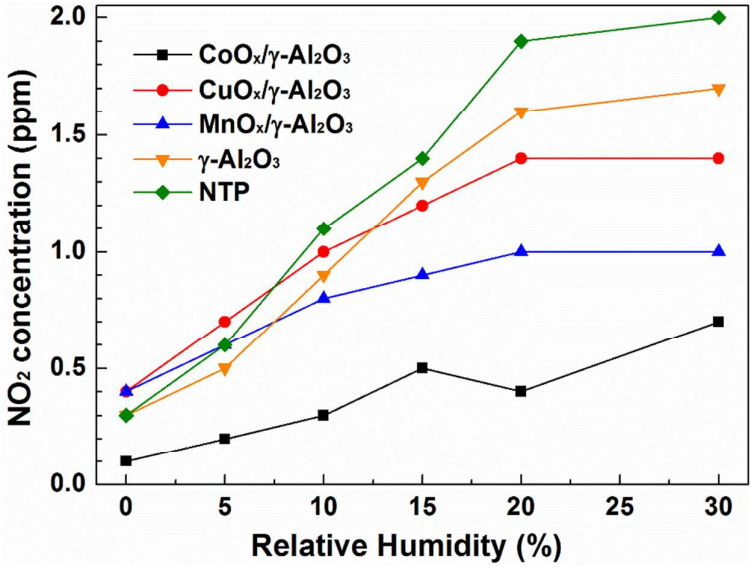

(a)

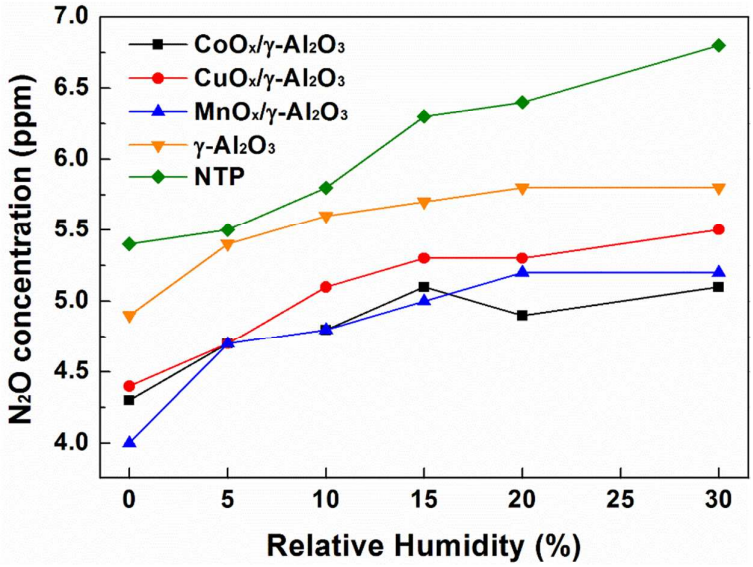

(b)

Fig. 7. Effect of RH on the concentration of NO_x (a) NO_2 and (b) N_2O.

The formation of nitrogen oxides (NO, NO_2 and N_2O) is not favourable in the removal of VOCs by dry or humid air plasmas.[63] These species are formed from reactions between excited oxygen and atomic nitrogen or excited nitrogen molecules. In this work, NO was not detected in all

the plasma reactions with and without catalyst. This could be attributed to the following two effects: first, using oxygen-rich carrier gases (e.g. 20% O_2 in this study), NO can be further oxidised to NO_2 via R14-R16, which has been confirmed by previous works;[42, 64] secondly, the presence of water in the air discharge could generate more OH radicals for the oxidisation of NO molecules into HNO_2.[65]

$$O_3 + NO \rightarrow NO_2 + O_2 \qquad \text{R14}$$

$$O + NO + M \rightarrow NO_2 + M \qquad \text{R15}$$

$$OH + NO \rightarrow HNO_2 \qquad \text{R16}$$

The effect of the RH and catalysts on the formation of NO_2 and N_2O in the plasma destruction of acetone is plotted in Fig. 7. The concentration of NO_2 is found to increase in the tested RH range of 0 - 30%, regardless of the catalyst used. For example, in the plasma reaction without catalyst, the formation of NO_2 increases from 0.3 to 2 ppm as the RH rises from 0 to 30% in the plasma destruction process. The combination of the plasma with $MO_x/\gamma\text{-}Al_2O_3$ catalysts significantly lowers the formation of NO_2 in the effluent compared to the plasma processing of acetone without catalyst or with $\gamma\text{-}Al_2O_3$ support. Similar findings were reported in previous works focused on the plasma-catalytic removal of other VOCs.[25] Hoard et al.[66] suggested the use of metal oxide catalysts can reduce the formation of NO_2. Okazaki et al.[67] found $\gamma\text{-}Al_2O_3$ supported metal oxide catalysts showed the most promising performance for NO_x reduction due to their activity and durability. These findings suggest that the surface reactions are responsible for the high NO_x removal efficiency, as the gas phase reactions do not justify the high NO_x removal efficiency. The catalytic effect could be attributed to the adsorption of NO_2 onto the catalyst surface, followed by the formation of NO_3^- as R17 and R18:[68]

$$3NO_2\,(g) + O_2^-\,(surf) \rightarrow 2NO_3^-\,(ads) + NO\,(g) \qquad \text{R17}$$

$$2NO_2\,(g) + O_2^-\,(surf) \rightarrow NO_3^-\,(ads) + NO_2^-\,(ads) \qquad \text{R18}$$

At a high RH (> 10%), the concentration of NO_2 is increased slightly or saturated, which can be attributed to the decreased adsorption of NO_2 onto the catalyst surface due to the blocking of

active sites by water molecules.

In addition, NO_2 is more water-soluble compared to NO and N_2O and could be absorbed by water in the humid air plasma. However, increasing the RH is found to form more NO_2. This phenomenon might be caused by the decreased catalytic activity due to the deactivation of the catalysts by water molecules. The catalytic adsorption has a more significant effect on the reduction of NO_2 formation compared to the absorption by water.

For the plasma destruction of acetone with and without catalyst, N_2O concentration increases slightly with increasing the RH, as shown in Fig. 7a. All the catalysts are found to reduce the formation of N_2O in the DBD. In the air plasma, N_2O is mainly formed from the reactions between excited nitrogen and oxygen atoms or from the reduction of NO_2. The presence of water vapor in the discharge generates OH radicals, which can react with NO_x to form HNO intermediates, followed by the recombination of HNO with itself to generate N_2O and H_2O.[69]

4. Conclusions

In this paper, the effect of air relative humidity on the decomposition of acetone in a dielectric barrier discharge reactor has been investigated in the absence and presence of MO_x/γ-Al_2O_3 (M = Co, Cu, or Mn) catalysts. It is found that increasing air humidity decreases the specific energy density of the discharge regardless the presence of the catalysts. The relative humidity of the carrier gas has also been identified as a critical parameter affecting the reaction performance of the plasma decomposition of acetone in terms of the removal efficiency, CO_2 selectivity, carbon balance and the formation of byproducts (e.g., ozone and NO_x). The presence of water in either plasma or plasma-catalysis systems has both positive and negative effects on the removal of acetone, depending on the content of water in the carrier gas. The maximum removal efficiency of acetone is achieved at the optimum relative humidity of 10% beyond which the removal rate of acetone decreases with increasing the RH, which can be attributed to the decrease of energetic electrons and the deactivation of catalysts due to the blocking of active sites on the catalysts in the plasma-

catalysis system. In addition, increasing air humidity enhances both CO_2 selectivity and carbon balance in the plasma processing of acetone with and without catalyst. However, we find that the presence of water in the plasma system slightly increases the formation of unwanted NO_2 and N_2O, but decreases the concentration of ozone. All the MO_x/γ-Al_2O_3 catalysts has played an important role in the improvement of carbon balance and CO_2 selectivity and reduction of unwanted byproducts.

Acknowledgement

Support of this work by National Science Fund for Distinguished Young Scholars (No. 51125025), National Natural Science Foundation of China (No. 51076140 & No. 51206143) and the Royal Society (UK) is gratefully acknowledged.

References

1 J. Williams and R. Koppmann, in *Volatile organic compounds in the atmosphere*, ed. R. Koppmann, Blackwell, 2007.
2 F. Holzer, *Appl. Catal. B: Environ*., 2002, 38, 163-181.
3 F. I. Khan and A. Kr Ghoshal, *J. Loss. Prevent. Proc*., 2000, 13, 527-545.
4 K. Urashima and J. S. Chang, *IEEE T. Dielect. El. In*., 2000, 7, 602-614.
5 J. Van Durme, J. Dewulf, C. Leys and H. Van Langenhove, *Appl. Catal. B: Environ*., 2008, 78, 324-333.
6 A. M. Vandenbroucke, R. Morent, N. De Geyter and C. Leys, *J. Hazard. Mater*., 2011, 195, 30-54.
7 H.H. Kim, *Plasma Processes Polym*., 2004, 1, 91-110.
8 R. Aerts, X. Tu, W. Van Gaens, J. C. Whitehead and A. Bogaerts, *Environ. Sci. Technol*., 2013, 47, 6478-6485.
9 X. Tu, H. J. Gallon and J. C. Whitehead, *J. Phys. D: Appl. Phys*., 2011, 44, 482003.
10 J. C. Whitehead, *Pure Appl. Chem*., 2010, 82, 1329-1336.
11 X. Tu and J. C. Whitehead, *Appl. Catal. B: Environ*., 2012, 125, 439-448.
12 X. Tu, H. J. Gallon and J. C. Whitehead, *Catal. Today*, 2013, 211, 120-125.
13 J. Karuppiah, E. L. Reddy, P. M. K. Reddy, B. Ramaraju and C. Subrahmanyam, *Int. J. Environ. Sci. Technol*., 2014, 11, 311-318.
14 H. H. Kim, A. Ogata and S. Futamura, *IEEE T. Plasma Sci*., 2006, 34, 984-995.
15 T. Hakoda, K. Matsumoto, A. Mizuno and K. Hirota, *Appl. Cataly. A: General*, 2009, 357, 244-249.
16 B. R. Raju, E. L. Reddy, J. Karuppiah, P. M. K. Reddy and C. Subrahmanyam, *J. Chem. Sci*., 2013, 125, 673-678.
17 J. H. Byeon, J. H. Park, Y. S. Jo, K. Y. Yoon and J. Hwang, *J. Hazard. Mater*., 2010, 175, 417-422.
18 A. S. Chiper, N. Blin-Simiand, M. Heninger, H. Mestdagh, P. Boissel, F. Jorand, J. Lemaire, J. Leprovost, S. Pasquiers, G. Popa and C. Postel, *J. Phys. Chem. A*, 2010, 114, 397-407.
19 S. Chavadej, K. Saktrakool, P. Rangsunvigit, L. L. Lobban and T. Sreethawong, *Chem. Eng. J*., 2007, 132, 345-353.
20 M. Schiorlin, E. Marotta, M. Rea and C. Paradisi, *Environ. Sci. Technol*., 2009, 43, 9386-9392.
21 H. B. Huang, D. Ye and D. Y. C. Leung, *IEEE T. Plasma Sci*., 2011, 39, 877-882..
22 F. Thevenet, L. Sivachandiran, O. Guaitella, C. Barakat and A. Rousseau, *J. Phys. D: Appl. Phys.*, 2014, 47, 224011.
23 T. Zhu, J. Li, Y. Jin, Y. Liang and G. Ma, *Int. J. Environ. Sci. Technol.*, 2008, 5, 375-384.
24 H. Huang, D. Ye and D. Y. C. Leung, *IEEE T. Plasma Sci*., 2011, 91, 576-580.
25 X. Fan, T. Zhu, Y. Wan and X. Yan, *J. Hazard. Mater.*, 2010, 180, 616-621.
26 J. Wu, Q. Xia, H. Wang and Z. Li, *Appl. Catal. B: Environ.*, 2014, 156-157, 265-272.
27 M. Sugasawa, T. Terasawa and S. Futamura, *IEEE T. Ind. Appl.*, 2010, 46, 1692-1698.
28 M. N. Lyulyukin, A. S. Besov and A. V. Vorontsov, *Plasma Chem. Plasma P.*, 2010, 31, 23-39.
29 C. L. Chang and T. S. Lin, *Plasma Chem. Plasma P.*, 2005, 25, 227-243.

30 L. Sivachandiran, F. Thevenet, P. Gravejat and A. Rousseau, *Chem. Eng. J.*, 2013, 214, 17-26.
31 R. Rudolph, K. P. Francke and H. Miessner, *Plasma Chem. Plasma P.*, 2002, 22, 401-412.
32 G. J. M. Hagelaar and L. C. Pitchford, *Plasma Sources Sci. Technol.*, 2005, 14, 722-733.
33 S. Pancheshnyi, S. Biagi, M. C. Bordage, G. J. M. Hagelaar, W. L. Morgan, A. V. Phelps and L. C. Pitchford, *Chem.Phys.*, 2012, 398, 148-153.
34 A. Phelps and L. Pitchford, *Phys. Rev. A*, 1985, 31, 2932-2949.
35 B. Eliasson and U. Kogelschatz, *J. Phys. B: Atom. Mol. Phys.*, 1986, 19, 1241-1247.
36 Y. Itikawa, *J. Phys. Chem. Ref. Data*, 2005, 34, 1.
37 R. Aerts, X. Tu, C. De Bie, J. C. Whitehead and A. Bogaerts, *Plasma Processes Polym.*, 2012, 9, 994-1000.
38 A. Fridman, *Plasma Chemistry*, Cambridge University Press, 2008.
39 C. Fitzsimmons, F. Ismail, J. C. Whitehead and J. J. Wilman, *J. Phys. Chem. A*, 2000, 104, 6032-6038.
40 R. Snoeckx, R. Aerts, X. Tu and A. Bogaerts, *J. Phys. Chem. C*, 2013, 117, 4957-4970.
41 S. E. Yin, B. M. Sun, X. D. Gao and H. P. Xiao, *Plasma Chem. Plasma P.*, 2009, 29, 421-431.
42 J. Van Durme, J. Dewulf, W. Sysmans, C. Leys and H. Van Langenhove, *Chemosphere*, 2007, 68, 1821-1829.
43 A. Y. Nikiforov, A. Sarani and C. Leys, *Plasma Sources Sci. Technol.*, 2011, 20, 015014.
44 A. S. Chiper, N. B. Simiand, F. Jorand, S. Pasquiers, G. Popa and C. Postel, *J. Optoelectron Adv. M.*, 2006, 8, 208-211.
45 L. Fouad and S. Elhazek, *J. Electrostat.*, 1995, 35, 21-30.
46 Z. Falkenstein and J. J. Coogan, *J. Phys. D: Appl. Phys*, 1997, 30, 817–825.
47 X. Tu, H. J. Gallon and J. C. Whitehead, *IEEE T. Plasma Sci.*, 2011, 39, 2172-2173.
48 J. S. Chang, Y. Uchida, K. Urashima and R. Taylor, *Plasma Processes Polym.*, 2006, 3, 721-726.
49 S. M. Saqer, D. I. Kondarides and X. E. Verykios, *Appl. Catal. B: Environ.*, 2011, 103, 275-286.
50 R. Vandenbrink, P. Mulder, R. Louw, G. Sinquin, C. Petit and J. Hindermann, *J. Catal.*, 1998, 180, 153-160.
51 A. Ogata, K. Yamanouchi, K. Mizuno, S. Kushiyama and T. Yamamoto, *IEEE T. Ind. Appl.*, 1999, 35, 1289-1295.
52 C. Subrahmanyam, A. Renken and L. Kiwi-Minsker, *Appl. Catal. B: Environ.*, 2006, 65, 157-162.
53 J. L. Wu, Y. X. Huang, Q. B. Xia and Z. Li, *Plasma Chem. Plasma P.*, 2013, 33, 1073-1082.
54 L. Magne, N. Blin-Simiand, K. Gadonna, P. Jeanney, F. Jorand, S. Pasquiers and C. Postel, *Eur. Phys. J.-Appl. Phys.*, 2009, 47.
55 S. Pasquiers, N. Blin-Simiand and L. Magne, *Plasma Phys. Contr. F.*, 2013, 55, 124023.
56 J. Van Durme, J. Dewulf, K. Demeestere, C. Leys and H. Van Langenhove, *Appl. Catal. B: Environ.*, 2009, 87, 78-83.
57 J. M. Wittbrodt, W. L. Hase and H. B. Schlegel, *J. Phys. Chem. B*, 1998, 102, 6539-6548.
58 X. Deng, T. Herranz, C. Weis, H. Bluhm and M. Salmeron, *J. Phys. Chem. C*, 2008, 112, 9668-9672.
59 C. Zheng, X. Zhu, X. Gao, L. Liu, Q. Chang, Z. Luo and K. Cen, *J. Ind. Eng. Chem.*, 2014, 20, 2761–2768.
60 J. Karuppiah, P. M. K. Reddy, E. L. Reddy and C. Subrahmanyam, *Plasma Processes Polym.*, 2013, 10, 1074-1080.
61 B. Dhandapani and S. T. Oyama, *Appl. Catal. B: Environ.*, 1997, 11, 129-166.
62 J. Chen and J. H. Davidson, *Plasma Chem. Plasma P.*, 2002, 22, 495-522.
63 A. M. Harling, J. C. Whitehead and K. Zhang, *J. Phys. Chem. A*, 2005, 109, 11255-11260.
64 T. Yamamoto, C. L. Yang, M. R. Beltran and Z. Kravets, *IEEE T. Ind. Appl.*, 2000, 36, 923-927.
65 C. H. Zheng, X. Shen, X. Gao, Z. S. Li, X. B. Zhu, Z. Y. Luo and K. F. Cen, *IEEE T. Plasma Sci.*, 2013, 41, 485-493.
66 J. W. Hoard, T. J. Wallington, J. C. Ball, M. D. Hurley, K. Wodzisz and M. L. Balmer, *Environ. Sci. Technol.*, 1999, 33, 3427-3431.
67 N. Okazaki, Y. Shiina, H. Itoh, A. Tada and M. Iwamoto, *Catal. Lett.*, 1997, 49, 169-174.
68 E. Ozensoy, D. Herling and J. Szanyi, *Catal. Today*, 2008, 136, 46-54.
69 A. Mfopara, M. J. Kirkpatrick and E. Odic, *Plasma Chem. Plasma P.*, 2009, 29, 91-102.